molecular oral microbiology

molecular oral microbiology

VimA–dependent modulation of the secretome in *Porphyromonas gingivalis*

D. Osbourne[1], A.Wilson Aruni[1], Y. Dou[1], C. Perry[2], D.S. Boskovic[2], F. Roy[1] and H. M. Fletcher[1]

1 Division of Microbiology & Molecular Genetics, School of Medicine, Loma Linda University, Loma Linda CA, USA
2 Division of Biochemistry, School of Medicine, Loma Linda University, Loma Linda CA, USA

Correspondence: Hansel M. Fletcher, Division of Microbiology & Molecular Genetics, School of Medicine, Loma Linda University, Loma Linda, CA 92350, USA Tel.: +1 909 558 4472; fax: +1 909 558 4035; E-mail: hfletcher@llu.edu

Keywords: peptidoglycan sacculi; *Porphyromonas gingivalis* secretome; protein sorting
Accepted 6 July 2012
DOI: 10.1111/j.2041-1014.2012.00661.x

SUMMARY

The VimA protein of *Porphyromonas gingivalis* is a multifunctional protein involved in cell surface biogenesis. To further determine if its acetyl coenzyme A (acetyl-CoA) transfer and putative sorting functions can affect the secretome, its role in peptidoglycan biogenesis and effects on the extracellular proteins of *P. gingivalis* FLL92, a *vimA*-defective mutant, were evaluated. There were structural and compositional differences in the peptidoglycan of *P. gingivalis* FLL92 compared with the wild-type strain. Sixty-eight proteins were present only in the extracellular fraction of FLL92. Fifteen proteins present in the extracellular fraction of the parent strain were missing in the *vimA*-defective mutant. These proteins had protein sorting characteristics that included a C-terminal motif with a common consensus Gly-Gly–CTERM pattern and a polar tail consisting of aromatic amino acid residues. These observations suggest that the VimA protein is likely involved in peptidoglycan synthesis, and corroborates our previous report, which suggests a role in protein sorting.

INTRODUCTION

The secreted proteins of bacteria are important for their survival and can play a vital role in the organism's interaction with the host during the disease process. These proteins, some of which can be derived from bacterial cell surface components, may function in nutrient acquisition or enhance the pathogenic potential by facilitating host tissue colonization or by modulating the host cell responses including the immune response (Lamont & Jenkinson, 1998). *Porphyromonas gingivalis*, an important gram-negative periodontal pathogen, is known to possess several outer membrane structures and secreted proteins including capsule, polysaccharides, proteases, hemagglutinin, lipopolysaccharides, fimbriae and major outer membrane proteins that contribute to cell adherence and virulence (Watanabe *et al.*, 1992; Lamont & Jenkinson, 1998; Yoshimura *et al.*, 2008).

A key element in modulating the pathogenic potential of *P. gingivalis* is the post-translational modification of several of the major surface components. For example, the major proteases, called gingipains, consist of arginine-specific (Arg-gingipain [Rgp]) and lysine-specific (Lys-gingipain [Kgp]) proteases that are both extracellular and cell membrane associated. The maturation pathways of the gingipains are linked to the biosynthesis of surface carbohydrate moieties that are regulated by several proteins including the PorR (Shoji *et al.*, 2002), PorT (Sato, 2005; Nguyen *et al.*, 2009), Sov (Sato, 2005) VimA, VimE and VimF (Vanterpool *et al.*, 2004, 2005, 2006).

VimA is a 39-kDa protein that is encoded for by the *vimA* gene. This gene is part of the 6.15-kilobase *bcp-recA-vimA-vimE-vimF-aroG* locus. VimA plays a multifunctional role in *P. gingivalis.* In addition to the glycosylation and anchorage of several surface proteins including the gingipains, VimA can also modulate sialylation (Aruni *et al.*, 2011). A recent report also documented a role in acetyl coenzyme A (acetyl-CoA) transfer. In these studies, VimA was shown to modulate lipid A and its associated proteins and may be involved in protein sorting and transport (Aruni *et al.*, 2012).

The purified VimA protein in pull-down experiments interacted with several proteins (Vanterpool *et al.*, 2006; Aruni *et al.*, 2012). Common to many of these proteins were conserved secretory signals such as the TonB-dependent receptor (PG0707), hypothetical protein (PG0410) (Aruni *et al.*, 2012). The functional classifications of some of these proteins suggest an involvement in peptidoglycan and lipopolysaccharide synthesis. Several reports have suggested that an alteration or defect in the synthesis of the peptidoglycan layer and lipopolysaccharide can affect protein secretion (Bos & Tommassen, 2004). Although we cannot rule out that alteration in the cell surface may directly affect protein secretion, it remains unclear what role the *vimA* gene product may play in this process in *P. gingivalis*.

To further evaluate the role of VimA in protein sorting/trafficking in *P. gingivalis* we characterized the secretome of the *vimA*-defective mutant. The role of *vimA* in peptidoglycan synthesis was evaluated by assessing ultrastructure variations using atomic force microscopy, transmission electron microscopy and hydrolytic enzyme assays. Based on the data, the VimA protein is likely involved in peptidoglycan synthesis. In addition, a hypothesis that the *P. gingivalis* VimA protein is involved in protein post-translational modification, anchorage and sorting needed for proper secretion of several extracellular proteins is discussed.

METHODS

Bacterial strains and growth conditions

Porphyromonas gingivalis strains (W83, FLL92) were grown in either brain–heart infusion (BHI) broth (Difco Laboratories, Detroit, MI) supplemented with cysteine (0.1%), vitamin K (0.5 μg ml^{-1}) and hemin (5 μg ml^{-1}) (BHIKH) or in Trypticase Soy Broth containing menadione and hemin (TSBKH). Solid medium was prepared by supplementation with 1.5% agar and 5% defibrinated sheep blood (Hemostat Laboratories, Dixon, CA). All cultures, unless otherwise stated, were incubated at 37°C in an anaerobic chamber (Coy Manufacturing, Grass Lake, MI) in 80% N_2, 10% H_2 and 10% CO_2. Growth rates were determined spectrophotometrically at 600 nm (optical density).

Complementation of *vimA*

Polymerase chain reaction-mediated gene replacement was used to complement the *vimA* defect. In brief, the open reading frame of *vimA* was amplified using primers specific for the *vimA* gene. The amplified fragment was purified by agarose gel electrophoresis, then electroporated into electrocompetent FLL92 cells grown to log phase [optical density at 600 nm (OD_{600}) of 0.6). Electroporated cells were incubated for 12 h in 1 ml of broth followed by plating on BHIHK-blood plates. The plates were screened after 8 days for the presence of black-pigmented colonies. These colonies were evaluated subsequently for the presence of the uninterrupted *vimA* gene using polymerase chain reaction.

Peptidoglycan isolation from W83 and FLL92

Porphyromonas gingivalis peptidoglycan was prepared using the modified method previously reported by Ishii *et al.* (2010). In brief, 200 ml BHI broth cultures of *P. gingivalis* W83 and FLL92 were centrifuged (9000 ***g***, 10 min at 10°C), and the precipitates were resuspended in water. Trichloroacetic acid (10%) was added to the sample and the mixture was incubated at 4°C for 1 h. The sample was centrifuged (9000 ***g***, 5 min, at 10°C) then washed three times in water. The precipitate was incubated at 100°C for 1 h after being suspended in 50 mM sodium acetate buffer (pH 5.3) containing 8% sodium dodecyl sulfate (SDS). This was followed by an overnight incubation at room temperature. After centrifugation (43,000 ***g***, 1 h, 12°C), the sample was washed three times in water and resuspended in Tris–HCL containing 2% SDS and proteinase K (50 μg ml^{-1}) at 37°C for 12 h.

Preparation of murein sacculi

Murein sacculi were prepared from FLL92 and W83 using the method of Yao *et al.* (1999). Briefly, cells were grown to an OD_{600} of 0.7 representing log phase and 1.5–1.6 representing stationary phase in 2000 ml BHIKH media. These cultures were then centrifuged at 6000 ***g*** for 30 min, washed twice in phosphate-buffered saline (pH 7.0) containing 1 mM magnesium chloride, and then the pellet was resuspended with the same buffer. The suspension was then boiled in 2% weight/volume SDS for 3 h and left overnight at room temperature for 48 h, after which it was centrifuged for 1 h at 150,000 ***g*** (25°C) to pellet the sacculi. Sacculi were washed three times in deionized water at room temperature, then dialysed overnight in 1 l of deionized water.

Lytic enzyme assays

Several peptidoglycan hydrolytic enzymes, including muramidase (Sigma-Aldrich, St Louis, MO), and lysostaphin (Sigma) were used to determine the susceptibility of peptidoglycan and the murein sacculi to hydrolysis. In brief, peptidoglycan was suspended in 0.1 M potassium hydrogen phosphate (pH 7.3 to an approximate absorbance of 0.7 at 580 nm, in a 1-cm light path. Then, 100 $\mu g\ ml^{-1}$ of the enzyme was added to the peptidoglycan suspension at zero time and incubated at 37°C. The absorbance at 580 nm was followed for 24 h and the per cent hydrolysis was calculated using the absorbance of an untreated, peptidoglycan control (Barnard & Holt, 1985).

Microscopic examination

Atomic force microscopy (AFM) and transmission electron microscopy (TEM) were used to provide detailed visuals of the morphology of the murein sacculi. AFM was carried out using treated and untreated murein sacculi, isolated from W83 and FLL92 strains grown to stationary (OD 1.5–1.8) and exponential (OD 0.6–0.7) growth phases. Samples were washed twice in 0.1 M phosphate-buffered saline buffer pH 7.4 and mounted on a cover slide, then allowed to air dry. The AFM images were generated with a Multimode 8 scanning probe microscope (Bruker, Santa Barbara, CA) in the peak force^{TM} tapping mode and using ScanAsyst^{TM} (k = 0.4 Nm^{-1}, f = 70 kHz) air probes. Automated feedback parameter optimization was achieved using ScanAsyst^{TM}. The peak force^{TM} tapping mode modulates the cantilever at *c.* 2 kHz at each pixel of the image where the feedback is based on the interaction force each time the tip taps the sample. Images were captured in the height mode or peak force error (Pratto *et al.*, 2009).

The TEM was performed using the Philips Tecnai 12 TEM following the method of Hyatt (1991). Briefly, sacculi were absorbed to 400-mesh carbon and Formvar-coated EM grids. A drop of 2% (weight/volume) uranyl acetate was used to float the grid for 15 s to negatively stain the sample, this was followed by microscopy using a Philips Tecnai 12 operated under standard conditions with the cold trap in place (Yao *et al.*, 1999).

Bioinformatics analysis of VimA

The DNA and amino acid sequences were aligned using BIOEDIT (http://www.mbio.ncsu.edu/bioedit/bioedit.html). The signal peptide and potential cleavage sites were predicted using both the Neural network and the Hidden Markov Models (Johnson *et al.*, 2010). Signal peptide prediction and cleavage site prediction were performed using SIGNAL P 3.0 (Bendtsen *et al.*, 2004). Transmembrane helices were predicted using the TMHMM server (Krogh *et al.*, 2001). The post-translational modification pattern motifs were identified using the PPSEARCH tool *(*http://www.ebi.ac.uk/Tools/ppsearch*/)* (Kulikova *et al.*, 2004).

Cell fractionation

Extracellular fractions were prepared from cell-free culture fluid precipitated with 60% acetone (at −20°C) (Vanterpool *et al.*, 2006) from W83 and FLL92. The protein pellet was resuspended in 7 ml 100 mM Tris–HCl buffer (pH 7.4) in the presence of 1 mM *N-p*-tosyk-L-lysine chloromethyl ketone (TLCK), dialysed for 48 h against the same buffer then stored at −20°C until used.

Digestion of *P. gingivalis* wild-type and FLL92 proteins

Extracellular proteins were run on a 10% bis–Tris gel (Invitrogen, Carlsbad, CA) in 1 × MOPS running

buffer for 7.5 cm, then visualized by staining with SimplyBlue safe stain (Invitrogen) (Henry *et al.*, 2008). After destaining in water, the gel was cut into 1–2 mm slices. Gel slices were subsequently dehydrated in acetonitrile and dried in a vacuum centrifuge for 30 min. The gel slices were incubated for 1 h at 60°C in a solution containing 20 μl of 20 mM dithiothreitol in 100 mM NH_4HCO_3 (enough to cover the gel pieces). The dithiothreitol solution was replaced with an alkylating solution (20 μl of 200 mM iodoacetamide in 100 mM NH_4HCO_3) after cooling the proteins to room temperature. Gel slices were further incubated at ambient temperature for 30 min in the dark, followed by two washes with 150 μl of 100 mM NH_4HCO_3, then finely minced with a flame-sealed polypropylene pipette tip, dehydrated by the addition of acetonitrile, and vacuum dried. Following an overnight incubation of the gel pieces with 20 μl digestion buffer [1 μl of mass spectrometry (MS)-grade trypsin (http://www.promega.com) in 50 mM acetic acid with 1 μl of 100 mM NH_4HCO_3], the digestion reaction was stopped with 10 μl 5% formic acid. After transferring the digest solution (aqueous extraction) to a 0.65 ml siliconized tube, 30 μl 50% acetonitrile with 0.1% formic acid was added, the mixture was vortexed for 3 min, centrifuged and then sonicated for 5 min. The process was repeated and both extractions were pooled and concentrated to 10 μl in a vacuum centrifuge. Peptide extraction was accomplished using standard C_{18} ZipTip technology following the manufacturer's directions (Millipore, Bedford, MA).

MS and data analysis

An LCQ Deca XP Plus system (http://www.thermo.com) with nano-electrospray technology (http://www.newobjective.com) consisting of a reverse-phase C_{18} separation of peptides on a 10 cm by 75 μm capillary column using Microm Magic RP-18AQ resin (http://www.michrom.com) with direct electrospray injection was used to analyse the extracted peptides from each gel piece (Henry *et al.*, 2008). A four-part protocol was used for the MS and MS/MS analyses, this included one full MS analysis (from 450 to 1750 m/z) followed by three MS/MS events using data-dependent acquisition, where the most intense ion from a given full MS scan was subjected to collision-induced dissociation, followed by the second and third most intense ions. The nanoflow buffer gradient was extended over 45 min in conjunction with the cycle repeating itself every 2 s, using a 0–60% acetonitrile gradient from buffer B (95% acetonitrile with 0.1% formic acid) developed against buffer A (2% acetonitrile with 0.1% formic acid) at a flow rate of 250–300 nl min^{-1}, with a final 5 min 80% bump of buffer B before re-equilibration. To move the 20-μl sample from the autosampler to the nanospray unit, flow stream splitting (1 : 1000) and a Scivex 10 port automated valve (Upchurch Scientific, Oak Harbor, WA) together with a Michrom nanotrap column was used. The spray voltage and current were set at 2.2 kV and 5.0 μA, with a capillary voltage of 25 V in positive ion mode; 160°C was used as the spray temperature for peptides. Data collection was achieved using the XCALIBUR software (Thermo Scientific, West Palm Beach, FL, USA), then screened with BIOWORKS 3.1. MASCOT software (http://www.matrixscience.com) was used for each analysis to produce unfiltered data and output files. Statistical validation of peptide and protein findings was achieved using X TANDEM (http://www.thegmp.org) and SCAFFOLD 2 meta-analysis software (http://www.proteomesoftware.com). The presence of two different peptides at a probability of at least 95% was required for consideration as being positively identified. Confirmation of individual peptide matches was achieved using the BLAST database (http://www.oralgen.lanl.gov). The experiments were repeated twice and the results were analysed.

RESULTS

Complementation of the *vimA* defect in *P. gingivalis* FLL92

Inactivation of the *vimA* gene in *P. gingivalis* W83 resulted in a non-black-pigmented isogenic mutant, designated *P. gingivalis* FLL92, which showed reduced levels of proteolytic, hemagglutinating, hemolytic and sialidase activities and decreased resistance to oxidative stress (Abaibou *et al.*, 2001; Vanterpool *et al.*, 2005, 2006). This *vimA*-dependent phenotype was also observed in a different genetic background of *P. gingivalis* further supporting a possible multifunctional role for the VimA protein. To rule out the presence of other defects in *P. gingivalis* FLL92 that may contribute the observed phenotype, the inactivated *vimA* gene in this isogenic mutant

was replaced with the wild-type gene. Following electroporation of *P. gingivalis* FLL92 with the *vimA* open reading frame and incubation on blood agar plates for 5–10 days, several black-pigmented colonies (designated FLL92B, FLL92C and FLL92D) were identified. *Porphyromonas gingivalis* FLL92B and FLL92D were observed to have the similar characteristic phenotype as the wild-type W83 strain. The *P. gingivalis* FLL92C became hemolytic and black pigmented much later than wild-type W83 (+ 5 days) and autoaggregated when incubated in BHI broth. Notably, its gingipain activity was marginally higher than that of FLL92 in log phase. The *vimA* gene from this strain was sequenced to determine whether a mutation in the gene accounted for this phenotype. Two mutations were observed in FLL92C at positions 6 and 7, where CC was replaced by AG (results not shown). The translated product of this gene contained valine rather than isoleucine at the third amino acid position.

The murein sacculi from FLL92 differs from W83

In silico analysis of the VimA protein predicted a structure that showed similarity to the Fem family of proteins which in gram-positive bacteria are involved in cell envelope biogenesis, particularly in peptidoglycan formation (Brakstad & Maeland, 1997; Stapleton & Taylor, 2002; Mainardi *et al.*, 2008). Furthermore, the increased sensitivity of *P. gingivalis* FLL92 could suggest an alteration in the peptidoglycan layer (Osbourne *et al.*, 2010). The TEM and AFM were used to determine the morphology and topography of the peptidoglycan sacculi. The sacculi from *P. gingivalis* FLL92 mutant when compared with the wild-type was distinctly different, because it possessed a homogeneously uneven surface with numerous contours. Sacculi from *P. gingivalis* W83 were on average 100 nm longer than those observed in FLL92 (Figs 1 and 2). Murein sacculi from both strains were subsequently treated with 15 μg ml^{-1} of lysostaphin for 10 min and imaged via AFM (Fig. 3). Treated W83 were visibly different from the untreated control, as numerous contours were visible on the surface. In FLL92 mutant, the morphology of the treated sample was similar to the control.

Peptidoglycan from W83 is hydrolysed faster than FLL92

Modifications of peptidoglycans can affect their sensitivity to peptidoglycan hydrolases (Osbourne *et al.*, 2010). Several lytic enzymes including lysozyme and lysostaphin were used to determine whether the peptidoglycan of *P. gingivalis* FLL92 was chemically dissimilar to that of wild-type W83. No significant change was observed between the wild-type and FLL92 using lysozyme; however, with the lysostaphin-treated peptidoglycan, 75% of W83 peptidoglycan was hydrolysed at 17 min, compared with 58% of FLL92 at the same time-point (Fig. 4).

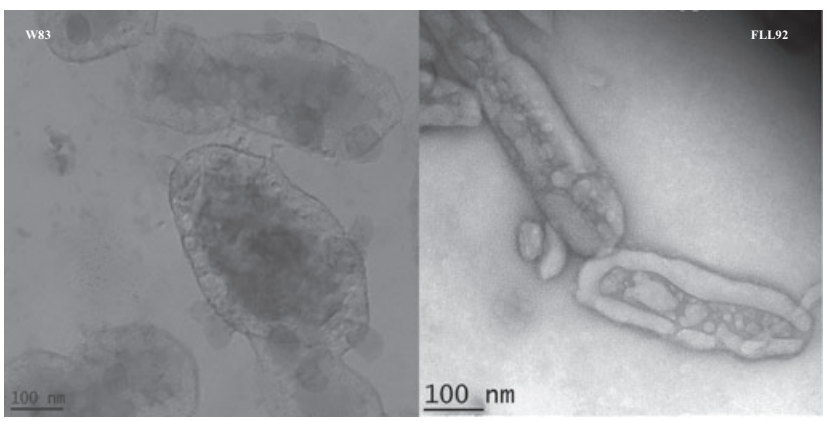

Figure 1 Muerin sacculus differs in FLL92 compared with wild-type. Transmission electron microscopy (TEM) was used to visualize the peptidoglycan sacculi of *Porphyromonas gingivalis* W83 and FLL92 strains, grown to 0.7 OD_{600}. Morphological differences were observed in FLL92, when compared with W83.

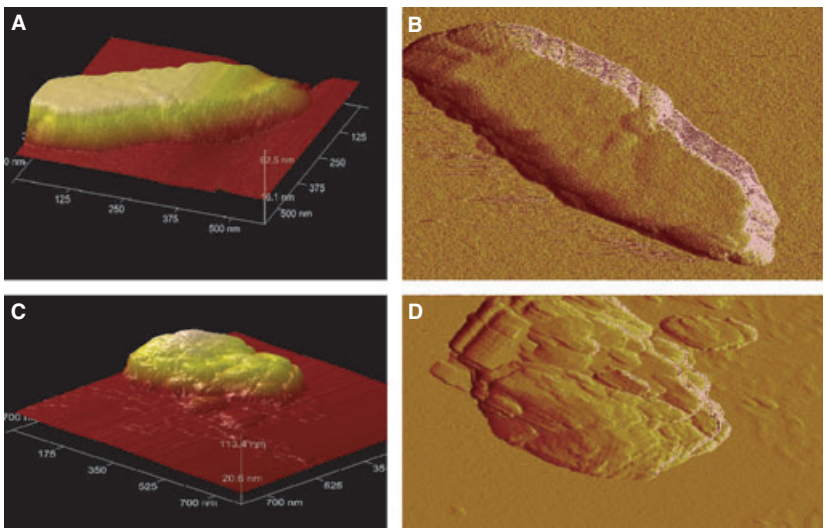

Figure 2 Sacculi toporaphy of W83 and FLL92. Atomic force microscopy (AFM) showing the peptidoglycan sacculi of *Porphyromonas gingivalis* W83 and FLL92 strains, grown to 0.7 OD_{600}. Morphological differences were observed in FLL92, when compared with W83. (A, B) *P. gingivalis* W83 sacculi, (C, D) *P. gingivalis* FLL92 sacculi.

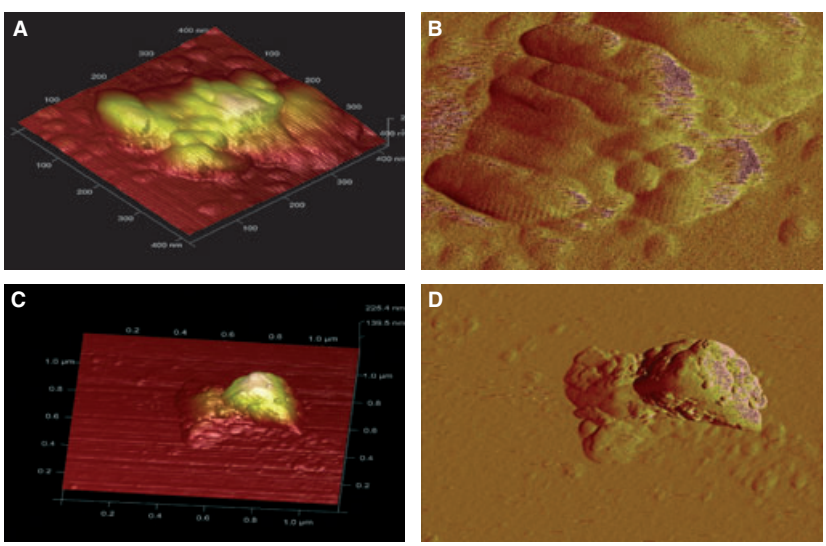

Figure 3 Sacculi of W83 and FLL92 after 10 min treatment with 16 μg ml^{-1} of Lysostaphin. Atomic force microscopy (AFM) showing the peptidoglycan sacculi of *Porphyromonas gingivalis* W83 and FLL92 strains, after 10 min of treatment with 16 μg ml^{-1} Lysostaphin. (A, B) *P. gingivalis* W83 sacculi after treatment, (C, D) *P. gingivalis* FLL92 sacculi after treatment.

VimA affects the secretion of several extracellular proteins

Mass spectrometric analysis was performed to determine whether the differential protein profile observed previously in FLL92 (Osbourne *et al.*, 2010), was unique to the membrane proteins or whether this mutation also affected the extracellular protein fraction. Mass spectrometry of extracellular fractions of W83 and FLL92 identified 68 proteins that were present in the extracellular fraction of FLL92 (Table 1) but absent in W83. Fifteen proteins that were present in the extracellular fraction of *P. gingivalis* W83 were missing in FLL92 (Table 2). Most of the aberrantly expressed proteins were predicted to be involved in energy metabolism, and the

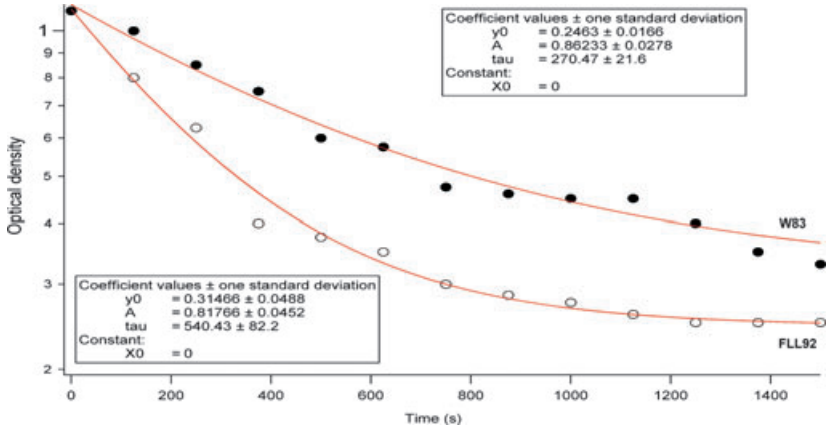

	W83 (17 min)	FLL92 (17 min)
Lysostaphin	75%	58%

Figure 4 Peptidoglycan from *Porphyromonas gingivalis* W83 is hydrolysed faster thatn FLL92 by Lysostaphin. Graph showing the hydrolysis of peptidoglycan sacculi of *P. gingivalis* W83 and FLL93 strains by lysostaphin. The test was performed in a BioRad microplate reader on a continuous mode.

remainder were predicted to be involved in proteolysis, protein binding and transport, DNA metabolism or were hypothetical. Of the 15 proteins identified as missing, six were predicted to play a role in cell envelope biogenesis; while two – PG0468 and PG1357 – were predicted to be involved in protein targeting and transport. Five of these proteins were hypothetical and two in amino acid metabolism. Seven extracellular proteins were identified in FLL92 as having spectral count values with negative fold changes (fc) of 1.2 or greater (Fig. 5): RgpA (PG1768, fc 1.2), Kgp (PG1605, fc 6.6), carboxypeptidase D (PG0212, fc 28), peptidylarginine deiminase (PG1249, fc 12.1), hemagglutinin (PG1602, fc 22.3), TonB-dependent OM receptor (PG0170, fc 285) and a hypothetical protein (PG0554, fc 50.7).

VimA alters the secretome of *P. gingivalis* and could be involved in protein sorting

In silico analysis of the missing protein in the extracellular fraction of *P. gingivalis* FLL92 was carried out to identify common motifs in the C-terminus of all the membrane proteins (both outer and inner membrane proteins). Out of the 15 missing proteins identified by mass spectrometry, nine proteins were found to be localized in the membrane of *P. gingivalis* (Table 3). The membrane proteins that were missing in *P. gingivalis* FLL92 were found to contain a strong N-terminal signal peptide with a C-terminal polar tail with aromatic residues at the end. Protein sequence alignment showed Gly-Gly-CTERM motif at positions 310 of all amino acids (Figs 6 and 7; see Fig. S1). A glycine-rich motif was noticed further down at positions 332–340. A common LxxxxG motif and DxGxTx motifs were present at the C-terminal end (Fig. 6).

On further analysis of the 15 FLL92 missing proteins, several common domains were identified (Table 4). Casein kinase II phosphorylation motifs, protein kinase C motifs and myristolation motifs were most abundant.

However, among the 68 aberrantly expressed proteins in FLL92, 14 were outer membrane proteins and three were periplasmic proteins. Only seven of the total membrane proteins had an N-terminal signal sequence. Multiple sequence alignment of these membrane proteins did not reveal any common consensus motif pattern except for the LxxxG motif (see Fig. S2). There were no Gly-Gly C-terminal motifs as noted in the FLL92 missing proteins.

Phylogram of VimA, FemA, FemB & FemX shows a close relationship of VimA to FemX

DISCUSSION

In this report, we have further clarified the multifunctional role of the VimA protein in *P. gingivalis*. The ability to restore the wild-type phenotype in

Table 1 Mass spectroscopy analysis of aberrantly expressed proteins in FLL92 extracellular fraction

Identified proteins (n = 68)	Accession no.	Putative role/function	Mol. wt	W83S.C.V	FLL92S.C.V
Hypothetical protein	PG0027	Unknown	25 kDa	0	2
UDP-3-*O*-acyl-GlcNAc deacetylase/ (3R)-hydroxymyristoyl-acp-dehydratase	PG0060	Fatty acid biosynthesis	52 kDa	0	3
Nitrogen assimilation regulatory protein (immunoreactive 47 kD antigen PG120)	PG0136	Transcription	47 kDa	0	12
Endothelin converting enzyme/neprilysin (PepO)	PG0146	Proteolysis	79 kDa	0	2
NADH oxidase/peroxidase	PG0160	Energy metabolism	104 kDa	0	7
Probable outer membrane protein (Omp85 analog)	PG0175	Cell envelope	102 kDa	0	5
Uroporphyrinogen-III synthase	PG0185	Biosynthesis of cofactors	28 kDa	0	7
Hypothetical protein	PG0227	Unknown	11 kDa	0	4
Translation initiation factor IF-2	PG0230	Translation	108 kDa	0	2
Conserved hypothetical protein	PG0264	Unknown	39 kDa	0	4
Polyferredoxin	PG0276	Energy metabolism	30 kDa	0	2
Probable dipeptidyl peptidase	PG0291	Proteolysis	101 kDa	0	2
Conserved hypothetical protein	PG0293	Unknown	15 kDa	0	3
DNA-mismatch repair protein	PG0350	DNA metabolism	95 kDa	0	9
DNA-directed RNA polymerase subunit beta	PG0360	Transcription	142 kDa	0	2
ATP-dependent DNA helicase	PG0381	DNA metabolism	82 kDa	0	4
ATP-dependent ClpX-related protease	PG0382	Proteolysis	46 kDa	0	16
Ferredoxin oxidoreductase beta subunit	PG0394	Energy metabolism	37 kDa	0	2
Conserved hypothetical protein	PG0411	Unknown	52 kDa	0	2
Conserved hypothetical protein	PG0452	Unknown	54 kDa	0	49
Pyruvate ferredoxin/flavodoxin oxidoreductase	PG0498	Energy metabolism	132 kDa	0	2
Hypothetical protein	PG0510	Hypothetical	34 kDa	0	5
Beta-galactosidase	PG0598	Energy metabolism	127 kDa	0	11
DNA topoisomerase I	PG0680	DNA metabolism	90 kDa	0	17
Acyl-CoA dehydrogenase (coenzyme A dehydrogenase)	PG0696	Metabolic process	65 kDa	0	2
Probable Xaa-Pro dipeptidase	PG0795	Proteolysis	44 kDa	0	4
Beta-galactosidase	PG0799	Energy metabolism	116 kDa	0	2
Translation elongation factor G protein	PG0832	Translation	80 kDa	0	2
Calcium ion-transporting ATPase	PG0838	Transport and binding	118 kDa	0	2
Threonyl-tRNA synthetase	PG0888	Translation	75 kDa	0	7
D-lysine 5,6-aminomutase alpha subunit	PG0955	Energy metabolism	57 kDa	0	6
Butyryl-CoA dehydrogenase	PG0958	Fatty acid metabolism	42 kDa	0	7
Alanine racemase; *N*-acetylymuramoylalanyl-D-glutamate-2, 6,-diaminopimelate-D-alanine-D-alanine ligase	PG0976	Cell envelope	92 kDa	0	2
Conserved hypothetical protein	PG0981	Unknown	107 kDa	0	9
Ribonucleotide reductase alpha subunit	PG1010	DNA replication	96 kDa	0	6
Probable long-chain fatty-acid-Coenzyme A ligase (long-chain acyl-CoA synthetase)	PG1028	Metabolic processing	69 kDa	0	3
Transferase protein	PG1029	Transposon functions	43 kDa	0	7
Xaa-Pro aminopeptidase	PG1071	Proteolysis	67 kDa	0	14
Hypothetical protein	PG1089	Unknown	80 kDa	0	17
GTP-binding protein (possible membrane protein)	PG1097	Signal transduction	66 kDa	0	2
Conserved hypothetical protein	PG1128	Unknown	47 kDa	0	5
Thiol protease (PrtT related)	PG1251	Proteolysis	93 kDa	0	2
O-succinylbenzoate–CoA ligase	PG1330	Biosynthesis of cofactors	40 kDa	0	9

Table 1 (continued)

Identified proteins (n = 68)	Accession no.	Putative role/function	Mol. wt	W83S.C.V	FLL92S.C.V
Magnesium-protoporphyrin *O*-methyltransferase; cobalamin biosynthesis protein N	PG1359	Biosynthesis of cofactors	163 kDa	0	2
Aminomethyltransferase (glycine cleavage system T protein)	PG1364	Energy metabolism	40 kDa	0	16
Nicotinate-nucleotide pyrophosphorylase (quinolinate phosphoribosyltransferase)	PG1377	Biosynthesis of cofactors	30 kDa	0	4
Bacteroides aerotolerance operon protein, batD	PG1385	Adaptations to atypical conditions	67 kDa	0	2
Fumarate reductase/succinate dehydrogenase flavoprotein subunit	PG1413	Energy metabolism	72 kDa	0	7
Cell division protein (ATPase)	PG1430	Cell division	96 kDa	0	2
Hypothetical protein	PG1448	Unknown	15 kDa	0	21
Conserved hypothetical protein	PG1496	Transport	99 kDa	0	2
ABC transporter, ATP-binding protein, MsbA family; MSD-NBD fusion protein	PG1497	Protein transport & binding	70 kDa	0	4
Hypothetical protein	PG1504	Protein binding	53 kDa	0	2
Immunoreactive 46 kDa antigen PG99	PG1572	Unknown	46 kDa	0	6
Enolase (phosphopyruvate hydratase) (2-phosphoglycerate dehydratase) (laminin binding protein)	PG1593	Energy metabolism	46 kDa	0	22
Urocanate hydratase	PG1630	Energy metabolism	74 kDa	0	2
Na^+/H^+-exchanging protein (Na^+/H^+ antiporter)	PG1634	Transport and binding	49 kDa	0	4
Polyphosphate kinase	PG1640	Polyphosphate biosynthesis	81 kDa	0	3
30S ribosomal protein S8	PG1677	Translation	15 kDa	0	4
30S ribosomal protein S3	PG1684	Translation	28 kDa	0	2
50S ribosomal protein L2	PG1687	Translation	30 kDa	0	3
30S ribosomal protein S7	PG1693	Translation	18 kDa	0	2
Hypothetical protein	PG1783	Cell redox, homeostasis	39 kDa	0	2
LPS-modified surface protein P59	PG1838	Cell envelope	61 kDa	0	38
Hypothetical protein	PG1867	Unknown	51 kDa	0	19
Hypothetical protein	PG1899	Hypothetical	27 kDa	0	6
Conserved hypothetical protein	PG1927	Unknown	214 kDa	0	3
Excinuclease ABC subunit A	PG1934	DNA metabolism	106 kDa	0	6

P. gingivalis FLL92 suggested that the observed multiple phenotype may result from a cascade of reactions or have a central mechanism. A non-black pigmented phenotype in *P. gingivalis* FLL92 could also be attributed to the missing Heme-binding protein (PG0602) (Dashper *et al.*, 2000) and its transport by the TonB-dependent receptor HumY (Wojtowicz *et al.*, 2009). In addition, glyceraldehyde-3-phosphate dehydrogenase, which is also one of the FLL92 missing proteins, is important in the glycolytic pathway and could affect glycosylation which could be important to the activation and anchorage of the gingipains (Abdel-Meguid *et al.*, 2008; Henderson & Martin, 2011). Similar to the phenotype of *P. gingivalis* FLL92, multiple reports have documented the phenotypic effects of altered gingipain activities in *P. gingivalis* (Potempa *et al.*, 1998; Curtis *et al.*, 1999, 2001; Lewis *et al.*, 1999; Veith *et al.*, 2002; Hasegawa *et al.*, 2003; Nakayama, 2003; Rangarajan *et al.*, 2005; Roy *et al.*, 2006; Kuboniwa *et al.*, 2009; Vanterpool *et al.*, 2010). Although it is likely that VimA-dependent glycosylation of the gingipains may be an important component in this process (Vanterpool *et al.*, 2006; Osbourne *et al.*, 2010), we cannot rule out other post-translational modifications.

VimA *in silico* analysis, predicts several domains, including one that is conserved among the acetyl-CoA *N*-acetyltransferase (Nat) superfamily and belongs to a broad family of proteins that includes the FemXAB (Schneider *et al.*, 2004) (Fig. S3a,b).

Table 2 Mass spectroscopy analysis of missing proteins in FLL92 extracellular fraction showing the spectral count values (SCV)

Identified proteins (n = 15)	Accession no.	Putative role/function	Mol. wt	W83S.C.V	FLL92S.C.V
Receptor antigen B	PG0171	Cell envelope	56 kDa	231	0
Conserved hypothetical protein	PG0375	Translation	144 kDa	5	0
Preprotein translocase subunit A protein	PG0468	Protein targeting	126 kDa	5	0
Glutamine-hydrolysing carbamoyl-phosphate synthase large subunit	PG0484	Arginine biosynthesis	120 kDa	3	0
Hypothetical protein	PG0552	Unknown	37 kDa	10	0
Hypothetical protein	PG0592	Unknown	45 kDa	29	0
Heme-binding protein/peripheral outer membrane chelatase	PG0602	Cell envelope	33 kDa	10	0
Outer membrane protein	PG0626	Cell envelope	42 kDa	10	0
TonB-dependent receptor HmuY	PG1357	Transport and binding	16 kDa	9	0
Probable integral outer membrane protein P20	PG1592	Cell envelope	24 kDa	2	0
Glyceraldehyde 3- phosphate dehydrogenase	PG1857	Energy Metabolism	36 kDa	2	0
Conserved hypothetical protein	PG1875	Unknown	123 kDa	3	0
Hypothetical protein	PG1894	Unknown	21 kDa	2	0
Outer membrane protein	PG1901	Cell envelope	32 kDa	7	0
Conserved hypothetical protein	PG1938	Unknown	61 kDa	7	0

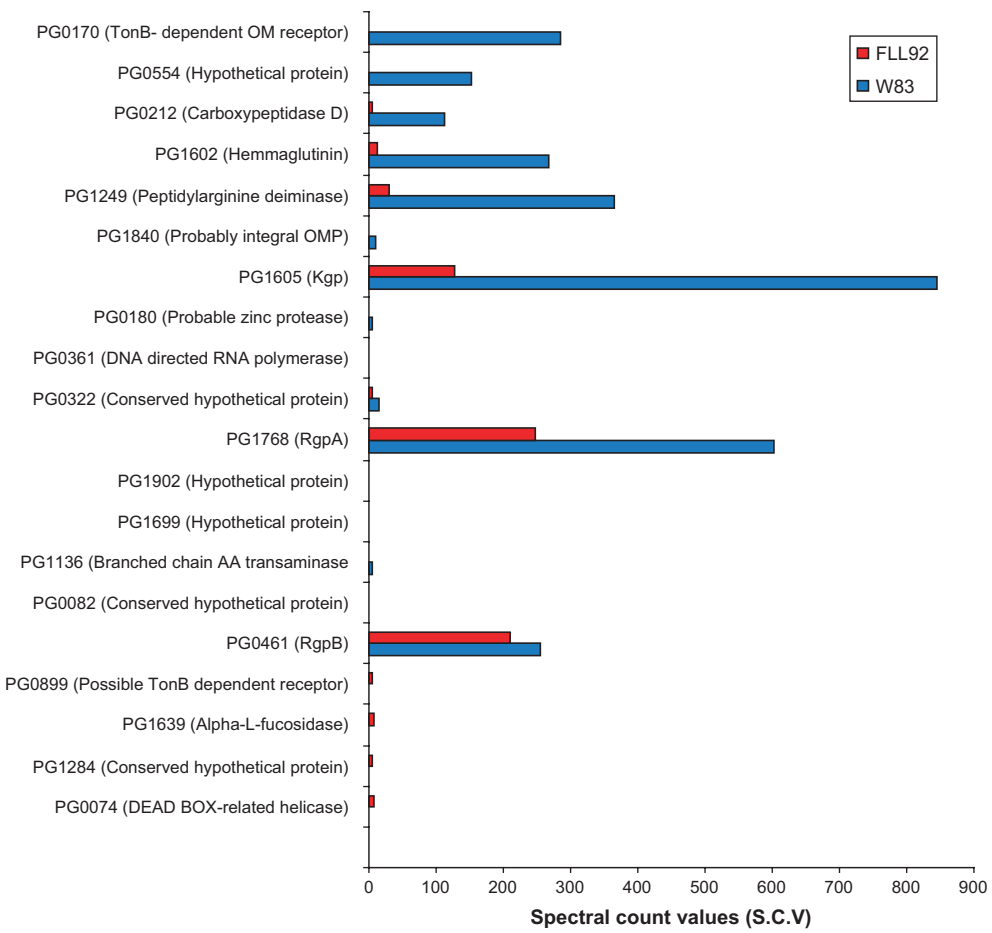

Figure 5 Extracellular proteins in *Porphyromonas gingivalis* strains with different spectral count values. Bar graph showing the variations in the spectral count of extracellular proteins between *P. gingivalis* FLL92 mutant and the wild-type W83.

Table 3 Mass spectroscopyanalysis of missing proteins in FLL92 extracellular fraction showing molecular characteristics of the proteins

Identified proteins (n = 15)	Lanl Accession no.	Putative role/function	Localization[1]	N-terminal signal peptide[2]	C-terminal polar tail	Mol. wt	W83. C.V	FLL92 S.C.V
Receptor antigen B	PG0171	Cell envelope	OM	Yes	Yes	56 kDa	231	0
Conserved hypothetical protein	PG0375	Translation	OM	Yes	Yes	144 kDa	5	0
Preprotein translocase subunit A protein	PG0468	Protein targeting	IM	No	Yes	126 kDa	5	0
Glutamine-hydrolysing carbamoyl-phosphate synthase large subunit	PG0484	Arginine biosynthesis	EC	No	No	120 kDa	3	0
Hypothetical protein	PG0552	Unknown	C	No	No	37 kDa	10	0
Hypothetical protein	PG0592	Unknown	OM	Yes	Yes	45 kDa	29	0
Heme-binding protein/peripheral outer membrane chelatase	PG0602	Cell envelope	PERI	Yes	Partial	33 kDa	10	0
Outer membrane protein	PG0626	Cell envelope	OM	Yes	Yes	42 kDa	10	0
TonB-dependent receptor HmuY	PG1357	Transport and binding	PERI			16 kDa	9	0
Probable integral outer membrane protein P20	PG1592	Cell envelope	OM	Yes	Yes	24 kDa	2	0
Glyceraldehyde 3-phosphate dehydrogenase	PG1857	Energy Metabolism	C	Yes	Yes	36 kDa	2	0
Conserved hypothetical protein	PG1875	Unknown	IM	Yes	Yes	123 kDa	3	0
Hypothetical protein	PG1894	Unknown	C	No		21 kDa	2	0
Outer membrane protein	PG1901	Cell envelope	OM	Yes	Yes	32 kDa	7	0
Conserved hypothetical protein	PG1938	Unknown	IM	Yes	Yes	61 kDa	7	0

[1]The subcellular localization was performed using Psort prediction server.
[2]The N-terminal signal sequence detection was performed using the iPsort.

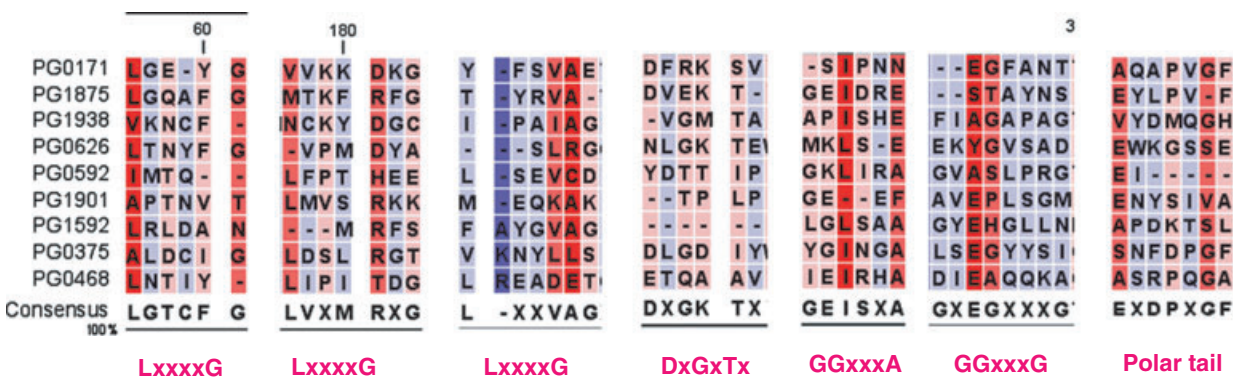

Figure 6 Multiple sequence alignment of the FLL92 missing proteins. Multiple sequence alignment of the FLL92 missing proteins using CLUSTALW was performed with nine out of 15 proteins which were membrane proteins and were found to have an N-terminal signal sequence. All the proteins showed a LxxxxG domain, DxGxTx domain and a polar tail with aromatic amino acid residues at the end.

The Fem family of proteins (Osbourne *et al.*, 2010; Aruni *et al.*, 2012) are known to be involved in cell envelope biogenesis, particularly peptidoglycan formation. Members of the FemABX family are novel ribosomal peptidyl transferases that are involved in the interchain peptide bridges of the peptidoglycan. Though primarily found in gram-positive bacteria they are also observed in a few gram-negative bacteria and spirochetes (Ghuysen, 1968; Hegde & Shrader, 2001). Our morphological studies showed variations in the sacculi of *P. gingivalis FLL92* compared with the wild-type strain. The presence or absence of

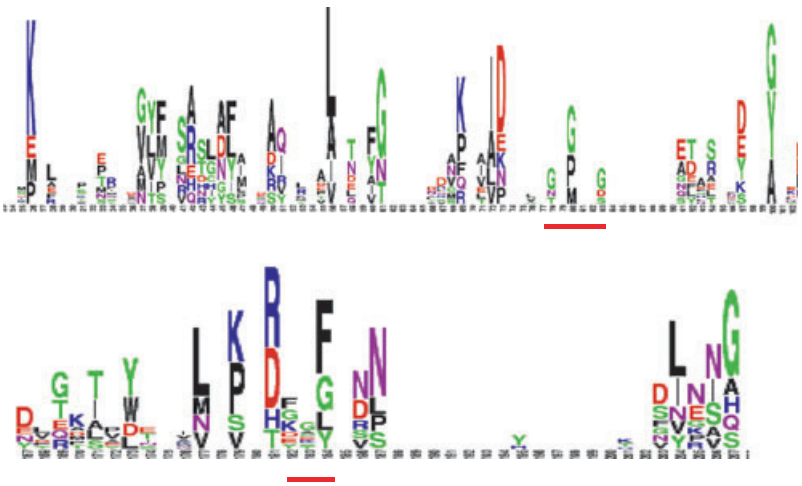

Figure 7 Sequence logo showing Gly-Gly-CTERM domain in the FLL92 missing proteins The presence of the Gly-Gly CTERM domain is underlined in red.

Table 4 Predicted post translational motifs in missing FLL92 extracellular proteins

Proteins	MYR	TYR_PHOS	CK2_PHOS	PKC_PHOS	CAMP_PHOS	ASN_GLYC	Amidationon	Unique
PG0171	4	0	6	0	0	2	0	0
PG0375	18	0	18	15	0	22	0	PTS-HPRRib S2
PG0468	7	0	20	23	3	4	4	ATP_GTP_ASECA
PG0484	15		17	7	1	3	0	CPSASE 1CPSASE 2
PG0552	6	1	3	1	0	1	0	0
PG0592	5	0	0	5	1	3	0	0
PG0602	3	0	2	4	0	2	0	0
PG0626	8	1	5	5	0	0	0	OMPA_1
PG1357	2	0	1	6	0	0	1	ATP_GTP_A
PG1592	8	0	2	4	0	1	0	0
PG1615	4	0	5	3	2	2	0	0
PG1857	7	0	8	5	1	3	0	GAPDH
PG1875	16	0	17	19	2	7	0	RGD
PG1894	5	1	1	0	0	0	1	0
PG1901	1	0	3	5	1	2	1	0
PG1938	23	0	5	8	0	4	0	0

MYR, *N*-myristoylation site; TYR_PHOS, tyrosine kinase phosphorylation site; CK2_PHOS, casein kinase II phosphorylation site; PKC_PHOS, protein kinase C phosphorylation site; CAMP_PHOS, cAMP and cGMP-dependent protein kinase phosphorylation site; ASN_GLYC, *N*-glycosylation site; Amidation, Amidation site; PTS-HPR, serine phosphorylation site signature; Rib S2, ribosomal protein S2 signature; SECA, SecA Family signature; ATP_HPR, ATP/GTP-binding site motif A; CPSASE 1, Carbamoyl-phosphate synthase subdomain signature 1; CPSASE 2, Carbamoyl-phosphate synthase subdomain signature 2; OMPA_1, OMPA-like domain; GAPDH, glyceraldehyde 3-phosphate dehydrogenase active site; RGD, cell attachment sequence.

acetyl moieties on the amino sugars in the peptidoglycans of some organisms can determine their sensitivity or resistance to several peptidoglycan hydrolases. Because of the similar sensitivity of the lysozyme, it is unlikely that the variation observed in *P. gingivalis FLL92* peptidoglycans is the result of acetylation of the amino sugars in the peptidoglycans (Reith & Mayer, 2011). Instead, the reduced ability of lysostaphin to hydrolyse the peptidoglycan from *P. gingivalis* FLL92 could indicate an alteration in the inter-peptide bridges (Grundling *et al.*, 2006). The amino acid composition of *P. gingivalis* tetrapeptide may contain alanine, diamino-pimelic acid (DAP), glycine and lysine (Barnard & Holt, 1985). Whereas

the amino acid composition of *P. gingivalis* FLL92 tetrapeptide is unknown, it is noteworthy that VimA has been shown to interact with alanyl tRNA synthetase (PG1101) (Vanterpool *et al.*, 2006; Aruni *et al.*, 2012) which, in other strains, can play a role in peptidoglycan synthesis. The ability to transfer an acetyl group from the acetyl-CoA to the amino group on the glucosamine-6-phosphate creating *N*-acetyl-glucosamine-6-phosphate is a major step in the synthesis of peptidoglycan (White, 2007). VimA has acetyl-CoA transfer function (Aruni *et al.*, 2012) and could be directly involved in peptidoglycan synthesis. Confirmation of a specific mechanism in this process is under further investigation.

VimA can modulate several surface-related structures including fimbriae, capsule and some outer membrane proteins (Osbourne *et al.*, 2010). In *P. gingivalis* some of these outer membrane surface proteins can become part of the secretome by a lipopolysaccharide-directed sorting mechanism (Haurat *et al.*, 2011). Results from this study have suggested that the secreted proteins are also altered in the *vimA*-defective mutant. Several proteins present in the extracellular fraction in FLL92 were missing from a similar *P. gingivalis* W83 fraction. It is noteworthy that PG1857 (glyceraldehyde-3-phosphate dehydrogenase), which is involved in the colonization of *P. gingivalis* (Nagata *et al.*, 2009), is the only protein that was found to be missing from both the membrane (Osbourne *et al.*, 2010) and extracellular fractions of FLL92. This could suggest defects in other secretory pathway(s)/mechanism(s). Of interest, PG1496 – a conserved hypothetical protein predicted to be involved in transport – is aberrantly expressed in the outer membrane (Vanterpool *et al.*, 2006) and extracellular fraction. Two other proteins with protein transport and binding functions, PG1497 and PG1504, were also aberrantly expressed. It is likely that these three proteins could be part of a novel transporter/cell-sorting system in *P. gingivalis* that, when disrupted, results in alterations in secretion and anchorage of proteins. It is also noteworthy that several cytoplasmic proteins were found in the extracellular fraction of FLL92, including those involved in energy metabolism, translation and DNA metabolism. Though we cannot definitively rule out the possibility of cytoplasmic contamination, the absence of other periplasmic/cyotplasmic markers (e.g. HtrA) likely suggests that some of the proteins found in the extracellular fraction of *P. gingivalis* FLL92 could be incorrectly targeted for secretion or their regulatory mechanism altered, so resulting in their secretion (Bohle *et al.*, 2011).

Several secreted proteins have primary and secondary structure similarity to the C-terminal domain of RgpB. These proteins have been designated the CTD family; and members of this family are attached to the cell surface through cell envelope glycans, which are important for proper folding and processing to produce a fully functional enzyme (Seers *et al.*, 2006). In contrast to the aberrantly expressed proteins, several of the missing extracellular proteins in *P. gingivalis* FLL92 did not conform to the C-terminal domain of RgpB CTD family but also carried an N-terminal signal peptide, a common C-terminal motif and a polar tail consisting of aromatic amino acids residues. Both the C-terminal motif with its common consensus Gly-Gly–CTERM pattern and polar tail are known to have protein sorting characteristics in other organisms (Ton-That *et al.*, 2004; Haft & Varghese, 2011). Because the VimA protein is predicted to have sorting signals (Aruni *et al.*, 2012), the unique C-terminal domain (CTD) with a glycine-rich region and a general sorting signal motif-like region (LxxxG) could be a general mechanism of VimA-mediated sorting for these missing proteins. It is unclear if there could be variation in VimA-mediated sorting. In a previous study (Aruni *et al.*, 2012), proteins interacting with VimA were also observed to carry a unique CTD motif pattern that was different from those in this study. In addition, the Gly-Gly-CTERM motif was not evident as noted in this study. However, the study showed both a common C-terminal glycine-rich domain that encompassed the sorting motif previously reported (Aruni *et al.*, 2012) and the Gly–Gly-CTERM motif noted in this study. It is unclear if there could be differential sorting possibly based on the association of VimA with other protein(s). Confirmation of a mechanism(s) is being actively investigated in the laboratory.

Taken together, our results further support the hypothesis that the *P. gingivalis* VimA protein is involved in protein post-translational modification, anchorage and sorting needed for proper secretion of several extracellular proteins. Preliminary observations in the laboratory suggest that VimA can modulate the acetylation profile in *P. gingivalis* (unpublished data). Acetylation is one of the most

common post-translational modifications in bacteria (Hu *et al*., 2010), and can affect protein sorting, cell-surface properties and morphology of important pathogens (Lee & Schneewind, 2001; Waksman *et al*., 2005; Laaberki *et al*., 2011). The multifunctional VimA (Abaibou *et al*., 2001; Vanterpool *et al*., 2004, 2005, 2006; Osbourne *et al*., 2010; Aruni *et al*., 2012) as a therapeutic target could have important implications for treatment strategies in controlling *P. gingivalis* infection.

ACKNOWLEDGEMENTS

This work was supported by Loma Linda University and Public Health Grant DE13664 and DE019730 from NIDCR (to HMF).

REFERENCES

Abaibou, H., Chen, Z., Olango, G.J., Liu, Y., Edwards, J. and Fletcher, H.M. (2001) *vimA* gene downstream of *recA* is involved in virulence modulation in *Porphyromonas gingivalis* W83. *Infect Immun* **69**: 325–335.

Abdel-Meguid, S.S., Von Der Helm, K., Korant, B.D. and Cheronis, J.C.D. (2008) *Proteases as Target for Therapy*, 2008 edn. Berlin Heidelberg: Springers-Verlag.

Aruni, W., Vanterpool, E., Osbourne, D. *et al.* (2011) Sialidase and sialoglycoproteases can modulate virulence in *Porphyromonas gingivalis*. *Infect Immun* **79**: 2779–2791.

Aruni, A.W., Lee, J., Osbourne, D. *et al.* (2012) VimA-dependent modulation of acetyl-CoA levels and lipid A biosynthesis can alter virulence in *Porphyromonas gingivalis*. *Infect Immun* **80**: 550–564.

Barnard, M.R. and Holt, S.C. (1985) Isolation and characterization of the peptidoglycans from selected gram-positive and gram-negative periodontal pathogens. *Can J Microbiol* **31**: 154–160.

Bendtsen, J.D., Nielsen, H., von Heijne, G. and Brunak, S. (2004) Improved prediction of signal peptides: SignalP 3.0. *J Mol Biol* **340**: 783–795.

Bohle, L.A., Riaz, T., Egge-Jacobsen, W. *et al.* (2011) Identification of surface proteins in *Enterococcus faecalis* V583. *BMC Genomics* **12**: 135.

Bos, M.P. and Tommassen, J. (2004) Biogenesis of the gram-negative bacterial outer membrane. *Curr Opin Microbiol* **7**: 610–616.

Brakstad, O.G. and Maeland, J.A. (1997) Mechanisms of methicillin resistance in staphylococci. *APMIS* **105**: 264–276.

Curtis, M.A., Thickett, A., Slaney, J.M. *et al.* (1999) Variable carbohydrate modifications to the catalytic chains of the RgpA and RgpB proteases of *Porphyromonas gingivalis* W50. *Infect Immun* **67**: 3816–3823.

Curtis, M.A., duse-Opoku, J. and Rangarajan, M. (2001) Cysteine proteases of *Porphyromonas gingivalis*. *Crit Rev Oral Biol Med* **12**: 192–216.

Dashper, S.G., Hendtlass, A., Slakeski, N. *et al.* (2000) Characterization of a novel outer membrane hemin-binding protein of *Porphyromonas gingivalis*. *J Bacteriol* **182**: 6456–6462.

Ghuysen, J.M. (1968) Use of bacteriolytic enzymes in determination of wall structure and their role in cell metabolism. *Bacteriol Rev* **32**: 425–464.

Grundling, A., Missiakas, D.M. and Schneewind, O. (2006) *Staphylococcus aureus* mutants with increased lysostaphin resistance. *J Bacteriol* **188**: 6286–6297.

Haft, D.H. and Varghese, N. (2011) GlyGly-CTERM and rhombosortase: a C-terminal protein processing signal in a many-to-one pairing with a rhomboid family intramembrane serine protease. *PLoS ONE* **6**: e28886.

Hasegawa, Y., Nishiyama, S., Nishikawa, K. *et al.* (2003) A novel type of two-component regulatory system affecting gingipains in *Porphyromonas gingivalis*. *Microbiol Immunol* **47**: 849–858.

Haurat, M.F., Aduse-Opoku, J., Rangarajan, M. *et al.* (2011) Selective sorting of cargo proteins into bacterial membrane vesicles. *J Biol Chem* **286**: 1269–1276.

Hegde, S.S. and Shrader, T.E. (2001) FemABX family members are novel nonribosomal peptidyltransferases and important pathogen-specific drug targets. *J Biol Chem* **276**: 6998–7003.

Henderson, B. and Martin, A. (2011) Bacterial virulence in the moonlight: multitasking bacterial moonlighting proteins are virulence determinants in infectious disease. *Infect Immun* **79**: 3476–3491.

Henry, L.G., Sandberg, L., Zhang, K. and Fletcher, H.M. (2008) DNA repair of 8-oxo-7,8-dihydroguanine lesions in *Porphyromonas gingivalis*. *J Bacteriol* **190**: 7985–7993.

Hu, L.I., Lima, B.P. and Wolfe, A.J. (2010) Bacterial protein acetylation: the dawning of a new age. *Mol Microbiol* **77**: 15–21.

Hyatt, A.D. (1991) *Electron Microscopy in Biology – A Practical Approach*. Oxford: Oxford University Press.

Ishii, K., Hamamoto, H., Imamura, K. *et al.* (2010) *Porphyromonas gingivalis* peptidoglycans induce excessive activation of the innate immune system in silkworm larvae. *J Biol Chem* **285**: 33338–33347.

Johnson, L.S., Eddy, S.R. and Portugaly, E. (2010) Hidden Markov model speed heuristic and iterative HMM search procedure. *BMC Bioinformatics* **11**: 431.

Krogh, A., Larsson, B., von Heijne, G. and Sonnhammer, E.L. (2001) Predicting transmembrane protein topology with a hidden Markov model: application to complete genomes. *J Mol Biol* **305**: 567–580.

Kuboniwa, M., Amano, A., Hashino, E. *et al.* (2009) Distinct roles of long/short fimbriae and gingipains in homotypic biofilm development by *Porphyromonas gingivalis*. *BMC Microbiol* **9**: 105.

Kulikova, T., Aldebert, P., Althorpe, N. *et al.* (2004) The EMBL nucleotide sequence database. *Nucleic Acids Res* **32**: D27–D30.

Laaberki, M.H., Pfeffer, J., Clarke, A.J. and Dworkin, J. (2011) O-acetylation of peptidoglycan is required for proper cell separation and S-layer anchoring in *Bacillus anthracis*. *J Biol Chem* **286**: 5278–5288.

Lamont, R.J. and Jenkinson, H.F. (1998) Life below the gum line: pathogenic mechanisms of *Porphyromonas gingivalis*. *Microbiol Mol Biol Rev* **62**: 1244–1263.

Lee, V.T. and Schneewind, O. (2001) Protein secretion and the pathogenesis of bacterial infections. *Genes Dev* **15**: 1725–1752.

Lewis, J.P., Dawson, J.A., Hannis, J.C., Muddiman, D. and Macrina, F.L. (1999) Hemoglobinase activity of the lysine gingipain protease (Kgp) of *Porphyromonas gingivalis* W83. *J Bacteriol* **181**: 4905–4913.

Mainardi, J.L., Villet, R., Bugg, T.D., Mayer, C. and Arthur, M. (2008) Evolution of peptidoglycan biosynthesis under the selective pressure of antibiotics in gram-positive bacteria. *FEMS Microbiol Rev* **32**: 386–408.

Nagata, H., Iwasaki, M., Maeda, K. *et al.* (2009) Identification of the binding domain of *Streptococcus oralis* glyceraldehyde-3-phosphate dehydrogenase for *Porphyromonas gingivalis* major fimbriae. *Infect Immun* **77**: 5130–5138.

Nakayama, K. (2003) Molecular genetics of *Porphyromonas gingivalis:* gingipains and other virulence factors. *Curr Protein Pept Sci* **4**: 389–395.

Nguyen, K.A., Zylicz, J., Szczesny, P., Sroka, A., Hunter, N. and Potempa, J. (2009) Verification of a topology model of PorT as an integral outer-membrane protein in *Porphyromonas gingivalis*. *Microbiology* **155**: 328–337.

Osbourne, D.O., Aruni, W., Roy, F. *et al.* (2010) The role of vimA in cell surface biogenesis in *Porphyromonas gingivalis*. *Microbiology* **156**: 2180–2193.

Potempa, J., Mikolajczyk-Pawlinska, J., Brassell, D. *et al.* (1998) Comparative properties of two cysteine proteinases (gingipains R), the products of two related but individual genes of *Porphyromonas gingivalis*. *J Biol Chem* **273**: 21648–21657.

Pratto, F., Suzuki, Y., Takeyasu, K. and Alonso, J.C. (2009) Single-molecule analysis of protein–DNA complexes formed during partition of newly replicated plasmid molecules in *Streptococcus pyogenes*. *J Biol Chem* **284**: 30298–33306.

Rangarajan, M., Hashim, A., duse-Opoku, J., Paramonov, N., Hounsell, E.F. and Curtis, M.A. (2005) Expression of Arg-gingipain RgpB is required for correct glycosylation and stability of monomeric Arg-gingipain RgpA from *Porphyromonas gingivalis* W50. *Infect Immun* **73**: 4864–4878.

Reith, J. and Mayer, C. (2011) Characterization of a glucosamine/glucosaminide *N*-acetyltransferase of *Clostridium acetobutylicum*. *J Bacteriol* **193**: 5393–5399.

Roy, F., Vanterpool, E. and Fletcher, H.M. (2006) HtrA in *Porphyromonas gingivalis* can regulate growth and gingipain activity under stressful environmental conditions. *Microbiology* **152**: 3391–3398.

Sato, K. (2005) Identification of a new membrane-associated protein that influences transport/maturation of gingipains and adhesins of *Porphyromonas gingivalis*. *J Biol Chem* **280**: 8668–8677.

Schneider, T., Senn, M.M., Berger-Bachi, B., Tossi, A., Sahl, H.G. and Wiedemann, I. (2004) *In vitro* assembly of a complete, pentaglycine interpeptide bridge containing cell wall precursor (lipid II-Gly5) of *Staphylococcus aureus*. *Mol Microbiol* **53**: 675–685.

Seers, C.A., Slakeski, N., Veith, P.D. *et al.* (2006) The RgpB C-terminal domain has a role in attachment of RgpB to the outer membrane and belongs to a novel C-terminal-domain family found in *Porphyromonas gingivalis*. *J Bacteriol* **188**: 6376–6386.

Shoji, M., Ratnayake, D.B., Shi, Y. *et al.* (2002) Construction and characterization of a nonpigmented mutant of *Porphyromonas gingivalis*: cell surface polysaccharide as an anchorage for gingipains. *Microbiology* **148**: 1183–1191.

Stapleton, P.D. and Taylor, P.W. (2002) Methicillin resistance in *Staphylococcus aureus*: mechanisms and modulation. *Sci Prog* **85**: 57–72.

Ton-That, H., Marraffini, L.A. and Schneewind, O. (2004) Protein sorting to the cell wall envelope of gram-positive bacteria. *Biochim Biophys Acta* **1694**: 269–278.

Vanterpool, E., Roy, F. and Fletcher, H.M. (2004) The vimE gene downstream of vimA is independently expressed and is involved in modulating proteolytic activity in *Porphyromonas gingivalis* W83. *Infect Immun* **72**: 5555–5564.

Vanterpool, E., Roy, F., Sandberg, L. and Fletcher, H.M. (2005) Altered gingipain maturation in vimA- and vimE-defective isogenic mutants of *Porphyromonas gingivalis*. *Infect Immun* **73**: 1357–1366.

Vanterpool, E., Roy, F., Zhan, W., Sheets, S.M., Sandberg, L. and Fletcher, H.M. (2006) VimA is part of the maturation pathway for the major gingipains of *Porphyromonas gingivalis* W83. *Microbiology* **152**: 3383–3389.

Vanterpool, E., Aruni, A.W., Roy, F. and Fletcher, H.M. (2010) regT can modulate gingipain activity and response to oxidative stress in *Porphyromonas gingivalis*. *Microbiology* **156**: 3065–3072.

Veith, P.D., Talbo, G.H., Slakeski, N. *et al.* (2002) Major outer membrane proteins and proteolytic processing of RgpA and Kgp of *Porphyromonas gingivalis* W50. *Biochem J* **363**: 105–115.

Waksman, G., Caparon, M. and Hultgren, S. (2005) *Structural Biology of Bacterial Pathogenesis*. Washington DC: ASM Press.

Watanabe, K., Yamaji, Y. and Umemoto, T. (1992) Correlation between cell-adherent activity and surface structure in *Porphyromonas gingivalis*. *Oral Microbiol Immunol* **7**: 357–363.

White, D. (2007) *The Physiology and Biochemistry of Prokaryotes*, 3rd edn. New York: Oxford University Press Inc.

Wojtowicz, H., Wojaczynski, J., Olczak, M., Kroliczewski, J., Latos-Grazynski, L. and Olczak, T. (2009) Heme environment in HmuY, the heme-binding protein of *Porphyromonas gingivalis*. *Biochem Biophys Res Commun* **383**: 178–182.

Yao, X., Jericho, M., Pink, D. and Beveridge, T. (1999) Thickness and elasticity of gram-negative murein sacculi measured by atomic force microscopy. *J Bacteriol* **181**: 6865–6875.

Yoshimura, F., Murakami, Y., Nishikawa, K., Hasegawa, Y. and Kawaminami, S. (2008) Surface components of *Porphyromonas gingivalis*. *J Periodontal Res* **44**: 1–12.

SUPPORTING INFORMATION

Additional supporting information may be found in the online version of this article:

Figure S1. The membrane proteins that were missing in *Porphyromonas gingivalis* FLL92 were found to contain a strong N-terminal signal peptide with a C-terminal polar tail with aromatic residues at the end. Protein sequence alignment showed Gly-Gly–CTERM motif at positions 310 of all amino acids.

Figure S2. Multiple sequence alignment of these membrane proteins did not reveal any common consensus motif pattern except for the LxxxG motif.

Figure S3. (a) Phylogram of VimA, FemA, FemB and FemX shows a close relationship of VimA to FemX. (b) Several consensus sequences are present in both VimA and FemX.

Please note: Wiley-Blackwell are not responsible for the content or functionality of any supporting materials supplied by the authors. Any queries (other than missing material) should be directed to the corresponding author for the article.